Renewable and Sustainable Energy Reviews 48 (2015) 1–16

Contents lists available at ScienceDirect

Renewable and Sustainable Energy Reviews

journal homepage: www.elsevier.com/locate/rser

Spatial interpolation and orographic correction to estimate wind energy resource in Venezuela

Francisco González-Longatt [a,*], Humberto Medina [b], Javier Serrano González [c]

[a] School of Electronic, Electrical and Systems Engineering, W2.63, Loughborough LE11 3TU, United Kingdom
[b] Faculty of Engineering & Computing, Coventry University, CV15FB Coventry, United Kingdom
[c] Department of Electrical Engineering, University of Seville, 41092 Seville, Spain

ARTICLE INFO

Article history:
Received 25 June 2014
Received in revised form
19 November 2014
Accepted 8 March 2015

Keywords:
Wind potential
Wind power
Wind resource assessment
Wind speed

ABSTRACT

This paper presents a wind resource assessment in Venezuela using an efficient combination of spatial interpolation and orographic correction for wind mapping. Mesoscale modelling offers a relatively accurate means to model meteorological conditions by solving the continuity and momentum equations. However, this approach is both time and computationally demanding. The methodology used in this work offers a computationally inexpensive solution by combining both a simple geo-statistical Kriging method to interpolate horizontal wind speed and an orographic correction to account for changes on terrain elevation. Hourly observations of wind speed and direction for 34 masts recorded during the period 2005–2009 have been analysed in order to define a statistical model of wind resources. The resulting method, which includes an exploratory statistical analysis of the wind data, is a computationally economical alternative to mesoscale modelling. Simulations results include equivalent mean wind speeds and wind power maps which have been created to a height of 50, 80 and 120 m above the ground based on a horizontal resolution of 15×15 km. Results show that the greatest wind energy resources are located in the coastal area of Venezuela with a potential for offshore applications. Preliminary findings provide a very positive evidence for offshore exploitation of wind power. Results also suggest that wind energy resources for commercial use (utility-scale) are available in northern Venezuela, additionally; they suggest excellent conditions for wind power production for micro-scale applications, both on- and off-grid.

Contents

* Corresponding author. Tel.: +44 150 9227061; fax: +44 150 9227475.
E-mail addresses: fglongatt@fglongatt.org (F. González-Longatt), aa7579@coventry.ac.uk (H. Medina), javierserrano@us.es (J. Serrano González).

http://dx.doi.org/10.1016/j.rser.2015.03.042
1364-0321/

1. Introduction

The Bolivarian Republic of Venezuela is located at the northernmost end of South America. It has a total surface area of 916,445 km^2 and a land area of 882,050 km^2. The country has a 2800-km coastline, (for more details see [1]). Venezuela is located within the latitude and longitude of 8°00′N and 66°00′W. Fig. 1 shows the internal political boundaries of Venezuela's 23 states. Four representative regions have been defined in this work: the West-Occidental region, the Central region, the South region (Los Llanos) and the East-Oriental region.

Venezuela has the largest electricity consumption in South America (4018 kW h/year per capita), and electrical power systems provide electricity to 95% of Venezuelan the population. Demand peak values vary between 16,500 MW and 18,200 MW depending on seasonal conditions. Electricity consumption rises between 4% and 7% per year, and it is expected to increase along similar lines during the next 10 years. Presently, the total installed power generation capacity in Venezuela is 26,550 MW, from which 65% extracted from hydropower, 32% from thermal power plants, and 3% from distributed energy resources. Although oil reserves in Venezuela are amongst the largest in the world, more aggressive policies on the use of environment friendly electricity generation have begun in recent years. Several academic projects have been reported to promote *renewable energy sources* (RES) installations in several areas of Venezuela [2–4], with a special focus on wind power exploitation. Gonzalez-Longatt et al. [3,4] have identified potential areas suitable for wind energy projects, including the Margarita island [3], the Paraguaná area [1], and the "La Guajira" area [5]. Several small-scale and off-grid wind power projects has been developed and two utility-scale wind farms are presently under development in mainland Venezuela: La Guajira (25 MW) [2], and La Peninsula de Paraguaná (100 MW) [1].

A wind speed map of Venezuela has been publicly available since 1960s, but there is limited information regarding its origin, quality and other relevant information to make this data reliable and/or useful. In last decade, Others wind maps have been developed using reanalysis [4], satellite data [6], and more recently, the Venezuelan Government has contracted LNEG—*Laboratório Nacional de Energia e Geologia* [7] to develop a full wind energy assessment and a wind map. However, this work has not yet been completed. Additionally, this work aims to bridge the gap between the limited on-site wind data (which is not publically available) and the need for an assessment of wind energy resources in Venezuela it can help stimulate and promote wind energy projects for the exploitation of wind resources for different applications, such as electricity generation, water pumping for irrigation, etc.

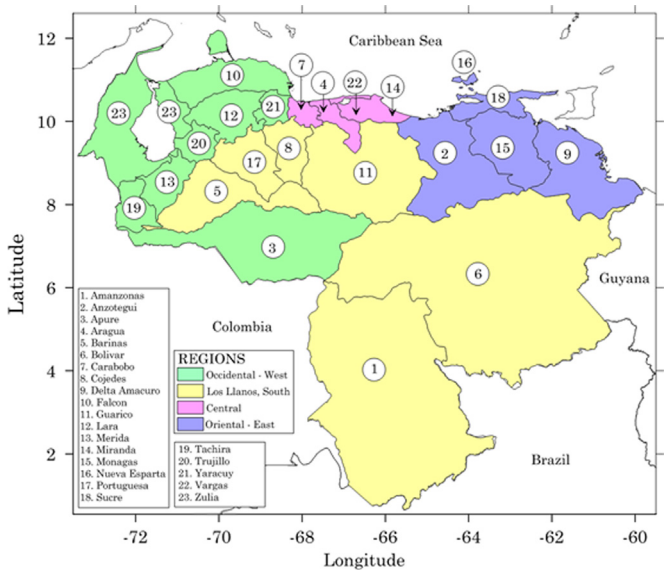

Fig. 1. Geographical location of Venezuela and political division.

Wind data are generally recorded at weather station locations, this information can be used for on-site wind energy assessments. However, wind resource mapping provides an indication of the wind resource across a very large area. Meso and micro wind assessments are used for national and local/site coverage. Mesoscale modelling is typically applied to describe wind resource with a horizontal resolution in the range of 1 km to 100 km. The methods used for mesoscale modelling typically resolve meteorological conditions within the modelling domain by solving the continuity and momentum equations to describe the atmosphere. There are several mesoscale modelling techniques and simulation programs dedicated to mesoscale modelling [8].

Wind resource assessment is a widely studied topic in the scientific literature. The wind conditions at specific locations have been analysed in several studies: Yaniktepe et al. [9] estimated the Weibull parameters in Osmaniye, Turkey, by a graphical method taking into account hourly time-series measured at the local meteorological station belonging to the Turkish State Meteorological Service. Mostafaeipour et al. [10] studied the wind energy feasibility for off-grid applications in the city of Shahrbabak, Iran. The research is based in the wind resource assessment by local measurements taken between 1997 and 2005. The wind resource in Port Said, Egypt, was featured by Lashin and Shata [11] by considering wind speed measurements performed in a mast of 19 m. Aman et al. [12] employed the data collected by the Pakistan Meteorological Department during four years in the city of Karachi, Pakistan, to assess the local resource. A similar study was conducted by Mpholo et al. [13] by analysing the wind resource in Masitise and Sani, Lesotho, taking into account the measurements obtained in local meteorological masts. Ozgener [14] presented the results acquired by the observations performed in Manisa, Turkey. The quality of wind resource in Masdar Citi, Abu Dhabi, was assessed by Janajreh et al. [15]. This study analysed the wind speed behaviour and turbulence taking into account the measurements performed at 50 m during 2010 with 10 min sample rate. Wu et al. [16] modelled and compared the performance of the three statistical distributions (Weibull, Lognormal and Logistic) used to model the wind behaviour by considering the data registered in a meteorological station in Inner Mongolia and Ben Amar et al. [17] modelled the wind behaviour by the Weibull and Rayleigh distributions at the location of the Sidi Daoud wind farm in Tunisia.

The wind resource over a specific area or region has also been presented in several scientific works: wind resource assessment was in the North coast of Senegal was presented by Youm et al. [18]. The authors evaluate the Weibull distribution and density power by analysing the data collected in five meteorological stations over

a period of two years. A similar research was presented by Tchinda et al. [19] for North Cameroon, wind speed frequencies measured in two meteorological masts are presented. Himri et al. [20,21] presented the results obtained at four meteorological stations located in Algeria. Wind speed and power density in Northern Mexico was presented by Hernández et al. [22]. The authors used Kriging method from ArcGIS v10 to interpolate the data collected in 221 meteorological stations.

Spatial interpolation is a computationally economical alternative to mesoscale modelling. This method was introduced by Palomino and Martin [23]. The method has been widely employed to estimate climate variables by the scientific community. Apaydin et al. [24] employed spatial interpolation for analysing solar radiation, sunshine duration, temperature, relative humidity, wind speed and rainfall in the region of the Southeastern Anatolia Project. Carrera and Gaskin [25] studied the distribution of climatological (rainfall and temperature) in the Basin of Mexico. Ninyerola et al. [26] applied spatial interpolation techniques to develop climatic cartography of precipitation in the Iberian Peninsula.

The estimation of wind energy resource by spatial interpolation has also been a recurrent topic in the existing literature. It has been successfully used to estimate wind energy resource in a wide range of coverage levels e.g. in-situ [27] and country level (e.g. England and Wales [28]). Yonga et al. [29] presented the wind map of Malaysia, Cellura et al. [30] analysed the wind resource in Sicily, Xydis et al. [31] studied the wind resource in Southern Greece, Liao et al. [32] conducted a similar study in China, Hossain et al. [33] studied the wind resource in India, Ali et al. [34] estimated the wind resource in Iran.

This paper presents a wind resource assessment in Venezuela based on spatial-interpolation and orographic correction of ground wind measurements. On-site observations from 34 meteorological stations have been used to create two main wind resource atlases, which have been generated at a height of 50, 80 and 120 m above the ground and they include both a traditional map of mean wind speeds (for each wind direction) and power density estimations.

This paper is organized as follows: Section 2 briefly describes the analysis method used to generate the wind resource map/s; Section 3 presents the input data used to perform the presented study. Section 4 presents the results obtained and their significance is discussed. Finally, in Section 5 conclusions of the analyses performed are provided.

The contributions of this paper are: (i) To demonstrate the potential for using wind energy resources commercially (utility-scale) in Venezuela, (ii) To identify wind electrical power and sites

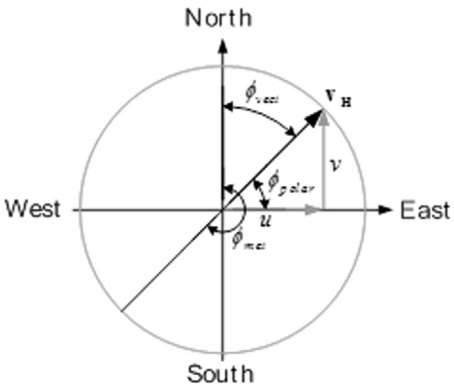

Fig. 3. Conventions used to represent the wind vector.

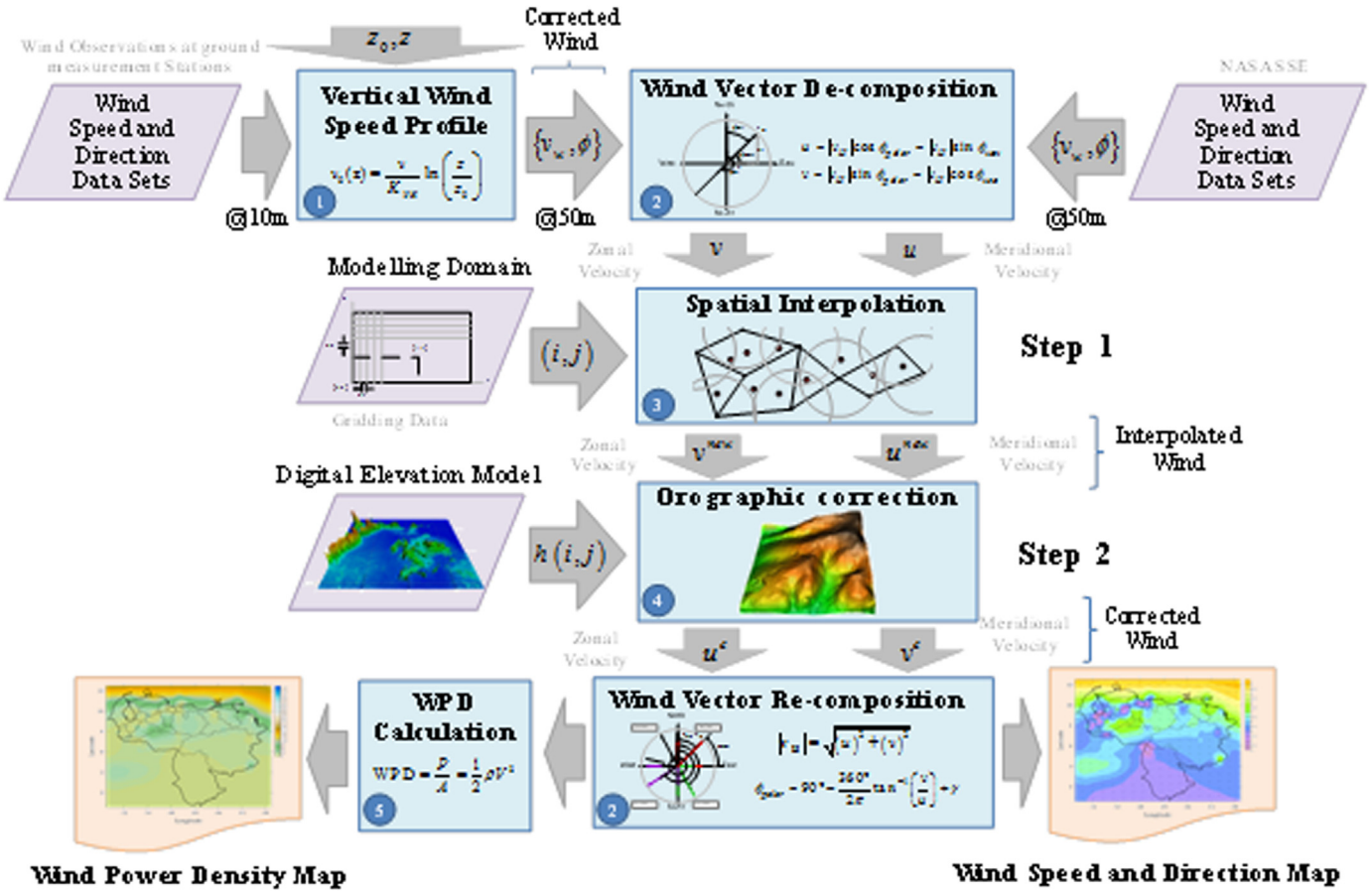

Fig. 2. Algorithmic framework used for the calculation of mean wind speeds and power density maps.

for commercial use onshore and (iii) To provide very positive evidence for offshore exploitation of wind power.

2. Analysis method

A regional assessment of wind and energy resources over a large area must predict the *mean wind speed* (m/s) and the *power density* (kW/m^2) (extractable wind energy) within the area considered. An observational wind resource mapping requires a model of the surface under consideration and description of wind energy resource in-situ.

Several methods have been developed to comprehensive set of the model for the horizontal and vertical extrapolation of wind data and the estimation of wind climate and wind resources.

This paper presents an algorithm to calculate surface wind-speed and direction considering changes in terrain high within the *atmospheric boundary layer* (ABL). The mean wind speed (m/s) and power density (kW/m^2) maps have been created using this algorithm and, an observational assessment of wind energy in Venezuela is presented.

The algorithm uses a two-step calculation procedure to estimate the wind speed and direction at each cell data of a high resolution grid: (i) *Step 1*: *spatial interpolation* is used for *horizontal extrapolation* of the data,(ii) *Step 2* applies an *orographic correction* in order to correct horizontal wind speeds due to terrain elevation changes. Fig. 2 presents a flowchart describing the calculation algorithm used in this paper. These steps are described in detail in the following subsections.

2.1. Vertical wind speed profile

The most widely used method for modelling the atmospheric boundary layer and extrapolating the wind speed from the height of observation to the height turbine hub is the *Prandtl logarithmic law* model under equilibrium conditions [35]:

$$v_0(z) = \frac{v}{K_{VK}} \ln\left(\frac{z}{z_0}\right) \tag{1}$$

where v is the friction velocity, K_{VK} is the Von Kármán constant (approximately 0.41), $v_0(z)$ is the mean wind speed at height z, and z_0 is the aerodynamic *roughness length*, in meters, which can vary by several orders of magnitude depending on whether smooth surfaces or cityscapes are being modelled.

2.2. Wind decomposition and re-composition

Azimuth representation is the classical way used in wind vanes to describe the physical direction of wind. Wind direction described by its azimuth is measured clockwise from the north from 0° to 360°. A wind of azimuth 200° blows from the SW and a wind of azimuth 45° blows directly from the NE.

A *wind vector* is used to describe the actual wind as the air flow moves and changes through both space and time. Consider a horizontal wind vector, $\mathbf{v_H}$, shown in Fig. 3.

The wind vector can be expressed in terms of *orthogonal velocity components* (see Fig. 3). Where u is the component of the horizontal wind towards East known as *Zonal Velocity* and v is the *Meridional Velocity* which represents the component of the horizontal wind towards the North. Fig. 3 shows three different conventions commonly used for wind direction:

- ϕ_{vect} is the wind *vector azimuth*, and it represents the direction *towards* which the wind is blowing. It increases clockwise from North when viewed from above. Terms such as northward, eastward etc. imply wind vector azimuths.
- ϕ_{met} is the *meteorological wind direction*. This reference is used to describe the direction *from* which the wind is blowing. It also increases clockwise from North when viewed on Fig. 3. Terms such as northerly, easterly etc. imply meteorological wind directions.
- ϕ_{polar} is the wind *vector polar angle* in two-dimensions. It increases anticlockwise from the positive x-axis, i.e. from East; this in the opposite sense to the wind vector azimuth and the meteorological wind direction, and uses a different origin.

The *direct de-composition* of the horizontal wind vector into zonal and meridional velocity is obtained using the following equations:

$$u = |\mathbf{v_H}| \cos\ \phi_{polar} = |\mathbf{v_H}| \sin\ \phi_{vect}$$
$$v = |\mathbf{v_H}| \sin\ \phi_{polar} = |\mathbf{v_H}| \cos\ \phi_{vect} \tag{2}$$

Fig. 4 shows wind vector de-composition including correspondence between the wind vector azimuth and wind vector polar angle.

An inverse transformation is used to *re-compose the wind components* (v, u) into the wind vector ($\mathbf{v_H}$). Using simple geometry, the magnitude of the vector, the wind speed ($|\mathbf{v_H}|$), is calculated as:

$$|\mathbf{v_H}| = \sqrt{(u)^2 + (v)^2} \tag{3}$$

The vector direction or wind direction is given by:

$$\phi_{polar} = 90° - \frac{360°}{2\pi} \tan^{-1}\left(\frac{v}{u}\right) + \gamma \tag{4}$$

where

$$\gamma = \begin{cases} 0° & u < 0 \\ 180° & u \geq 0 \end{cases} \tag{5}$$

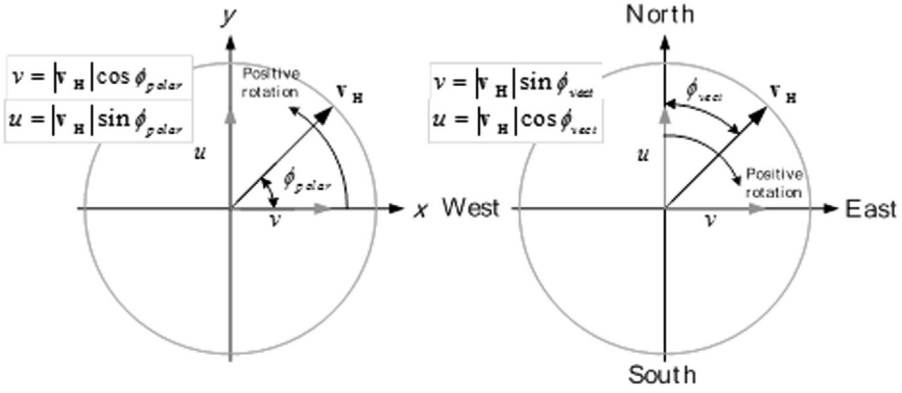

Fig. 4. Equivalence between vector azimuth and polar vector angle.

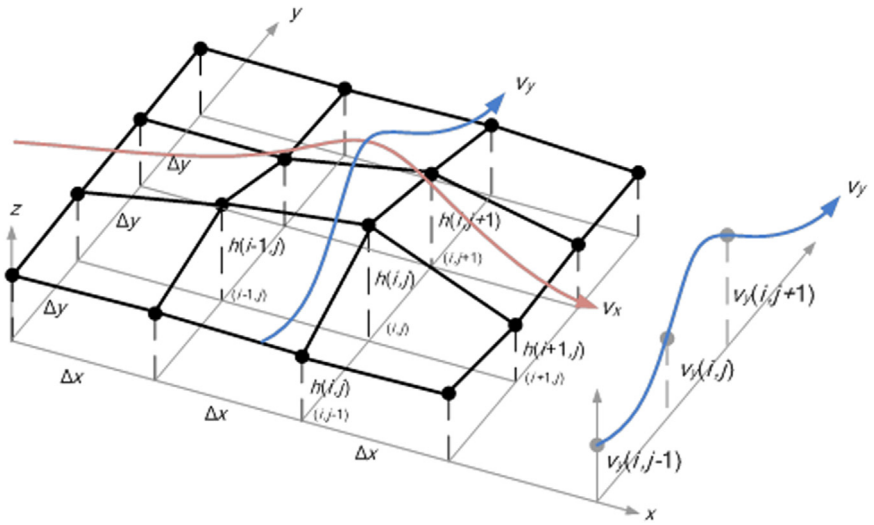

Fig. 5. Schematic showing the horizontal discretization around an arbitrary grid point (i, j) at height $h(i, j)$ whose velocity components $v_x(i, j)$ and $v_y(i, j)$ is calculated using the orographic correction.

2.3. Spatial interpolation

There are several methods used for numerical wind flow modelling [36]: mass-consistent, Jackson–Hunt, computational fluid dynamics (CFD), and mesoscale numerical weather prediction (NWP) models (e.g., MASS, WRF, ARPS, MC2, KAMM, etc.).

The PSU/NCAR mesoscale model (known as MM5) is a well-known model applied to numerical wind flow modelling. It is a limited-area, non-hydrostatic, terrain-following sigma-coordinate model designed to simulate or predict mesoscale atmospheric flows. MM5 uses the *Cressman scheme* for spatial interpolation. However, the main disadvantage of the MM5 is its relatively high computational demands.

Spatial interpolation can be used to interpolate wind fields between weather monitoring stations. This approach is not a common analysis methodology within the area of atmospheric computer models.

Geostatistical methods use sample points taken at different locations in a landscape and creates (interpolates) a continuous surface. They are based on statistical models that include autocorrelation, as a consequence, these techniques not only have the capability of producing a prediction surface but also provide a measure of the certainty or accuracy of the predictions. There are various geostatistical interpolation techniques from which the *Kriging methodo* describes a range of least squares methods to provide minimum variance linear unbiased predictions.

Kriging method assumes that the distance or direction between sample points reflects a spatial correlation that can be used to explain surface variations. The Kriging method is a multistep process which includes the following steps: (i) an exploratory statistical analysis of the data, (ii) *variogram modelling*, (iii) surface generation, and optionally, (iv) exploration of a variance surface. Kriging is most appropriate when there is a spatially correlated distance or directional bias in the data. Matheron's ordinary Kriging original formulation [37] is the most popular since it can be applied successfully in most situations and its assumptions can be easily satisfied [38]. It is more realistic than most other interpolation methods, and also more mathematically robust. The Kriging method is expressed using the following equation:

$$\hat{Z}(\mathbf{x}_0) = \sum_{i=1}^{N} \lambda_i z(\mathbf{x}_i) \tag{6}$$

where $z(\mathbf{x}_i)$ (for $i=1,2,\ldots,N$) are the observed values of variable z at points $\mathbf{x}_1,\mathbf{x}_2,\ldots,\mathbf{x}_N$, or in two dimensions $\mathbf{x}_i \equiv (x_{i1},x_{i2})^{\mathrm{T}}$, λ_i (for $i=1, 2,\ldots,N$) are the weights chosen to minimize the prediction error variance. The objective is to estimate/predict the value$\hat{Z}(\mathbf{x}_0)$. For a detailed derivation and discussion of the Kriging methodology see Cressie [39] or Journel and Huijbregts [40].

2.4. Orographic correction

The orographic correction is used to modify the horizontal wind velocity components based on the elevation differences from the horizontally interpolated terrain elevations. Several approaches can be adopted in order to perform a correction due to terrain orography. For example, mesoscale models [8], *Computational Fluid Dynamics* (CFD) [41,42], and methods using statistical-based corrections [43] have all been used successfully (to an extent) to perform orographic corrections. However, these techniques have not been adopted in this work, mainly, for two reasons. Firstly, techniques such as mesoscale models and CFD are computationally expensive, and secondly, statistics- or Bezier-based methods, whilst being less computationally expensive, can be difficult to implement and require user experience for the determination of model coefficients. Since the Venezuelan territory also has a complex topography, a method that is both computationally inexpensive and simple to implement was favoured [44].

The orographic correction of both horizontal velocity components v_x^{calc} and v_y^{calc} is determined by adding a correction calculated using the function f to the initially estimated velocity components v_x and v_y, see Eqs. (7) and (8), which result from the initial spatial interpolation of the measured wind speed datasets. It is known that even modest increases in terrain slope $\Delta h/\Delta x$ lead to increases in wind speed ([45] for a more recent review see [46]). Therefore, the function f is consequently used in order to include a correction due to terrain orography and it can be justified based on both the conservation of mass and the conservation of momentum principles applied to a streamline (see Fig. 5) where an increase in height Δh requires also an increase in velocity. The conservation of mass indicates that as the density decreases, as it is the case in atmospheric flows where all the state variables decrease with increasing altitude, the velocity must increase in order to maintain mass flow constant. Alternatively, the form adopted for the function f can be justified based on the conservation of momentum equation where the term $-\partial P/\partial x_i$ acts as a momentum sink if the pressure gradient increases in all spatial coordinates and as a source term if the pressure spatial gradient decreases as it is the case when the terrain altitude increases.

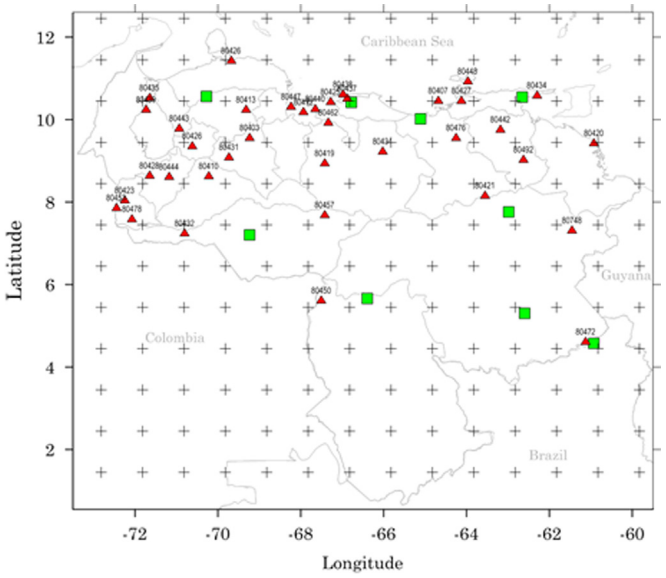

Fig. 6. Geographical location of weather stations (red triangle) and radars (green squares). Location of $1^\circ \times 1^\circ$ data obtained from the re-analysis dataset. (For interpretation of the references to color in this figure legend, the reader is referred to the web version of this article.)

However, for simplicity, the formulation of the function f assumes that pressure changes are linearly related to changes in height (Δh). Additionally, it is worth highlighting a favourable feature of the correction function f, that is, it is inversely proportional to the grid spacing (Δx and Δy). This has the effect of reducing the level of correction introduced by Eqs. (7) and (8) as the grid resolution is decreased which serves to minimise potential errors in the corrected wind velocity components for grids with insufficient or low density.

$$v_x^{\text{calc}} = v_x + f\left(\Delta h \frac{\Delta v_x}{\Delta x}\right) \tag{7}$$

$$v_y^{\text{calc}} = v_y + f\left(\Delta h \frac{\Delta v_y}{\Delta y}\right) \tag{8}$$

Finally, the orographic correction is implemented using a central difference calculation (see Fig. 5) around the grid node for which the velocity is to be corrected and the corrected velocity components (v_x^{calc} and v_y^{calc}) are calculated using the equations:

$$v_x^{\text{calc}} = v_x + \frac{1}{2}\left[\frac{(h(i,j)-h(i-1,j))(v_x(i-1,j)-v_x(i,j))}{\Delta x} + \cdots \right.$$
$$\left. \cdots + \frac{(h(i+1,j)-h(i,j))(v_x(i,j)-v_x(i+1,j))}{\Delta x}\right] \tag{9}$$

$$v_y^{\text{calc}} = v_y + \frac{1}{2}\left[\frac{(h(i,j)-h(i-1,j))(v_y(i-1,j)-v_y(i,j))}{\Delta y} + \cdots \right.$$
$$\left. \cdots + \frac{(h(i+1,j)-h(i,j))(v_y(i,j)-v_y(i+1,j))}{\Delta y}\right] \tag{10}$$

2.5. Wind power density (WPD)

The *wind power density* (WPD) is calculated based on the following equation [35]:

$$\text{WPD} = \frac{P}{A} = \frac{1}{2}\rho V^3 \tag{11}$$

where P/A is the wind power density, or power per unit area (W/m^2), ρ is the air density (kg/m^3) and V is the average wind speed within the time span considered (m/s). Observation time-scale patterns (daily, weekly, monthly, etc.) are included in the WPD estimation using the *energy pattern factor*, K_E [47]:

$$K_E = \frac{\text{total ammount of power available in the wind}}{\text{power calculated by tje cubinh the mean wind speed}} \tag{12}$$

Given set of N hourly data V_n, K_E is defined as:

$$K_E = \frac{\frac{1}{N}\sum_{i=1}^{N} V_i^3}{\left(\frac{1}{N}\sum_{i=1}^{N} V_i\right)^3} \tag{13}$$

The energy pattern factor K_E itself is used to indicate the wind potential of a given site by means of its power density

$$\text{WPD} = \frac{P}{A} = K_E \frac{1}{2}\rho V^3 \tag{14}$$

3. Source data

In this section, the data used to create the wind resource atlas of Venezuela is presented. Data consists of two subsets used as inputs to the calculation algorithm (described in Section 2—see Fig. 2) statistical description of the wind data and topography data or elevation model. The two primary model inputs are *digital terrain data* and *wind data.*

3.1. Wind data

High-quality surface wind data from well-exposed locations can provide the best statistical description of the wind resources available for the region of interest. In this paper, quality ground measurement data is used together with re-analysis data to fill the gap where ground measurements are missing, and to augment areas where ground measurements do exist. The long-term overall statistics based on the re-analysis dataset is used in combination with nearly three years' worth of surface station observations. The following sections present a summary of the surface data sets used.

3.1.1. Surface station observations

The single most important data sources for the calculation algorithm are surface stations. Venezuela has a weather station network across the whole Venezuelan territory. It has 5 radars and more than 300 weather stations, the majority of meteorological stations belonging to the *National Institute of Meteorology and Hydrology* [48] and 37 stations belonging to *Meteorology Service of the Venezuelan Air Force* (MSVAF) [49] (see Fig. 6). The weather stations are located in both rural and urban sites, mainly in airports and military bases. Table 1 shows a summary of historical wind speed and direction data for 34 stations, consisting of mean monthly wind speeds for each year of record.

These weather stations collect temperature, wind speed, wind direction, humidity, rainfall, atmospheric pressure, solar isolation, and other climatic variables. Although the distribution of stations is biased towards valley locations, where main military installations and airports are located, there is a sufficient number of mountain stations to construct three-dimensional correction fields to the numerical wind flow model output, based on observations.

The station density versus elevation roughly corresponds to the area-height distribution of the topography up to about 666 m. At higher elevations, the station density is lower than it ideally should be according to the area-height distribution. There are only two stations over 1000 m above sea level (mamsl) located in the Andes Mountains i.e. Mérida-80438 and Palmichal-80748.

3.1.2. Reanalysis data

Reanalysis data has been obtained from the NASA Langley Research Center of Atmospheric Science Data Center Surface

Table 1
Description and geographical coordinates of weather stations in Venezuela coordinated by MSVAF.

Code	Station name	Geographical coordinates		Elevation (m above sea level)	Register period	Yearly average wind speed (m/s)	Yearly average wind power density (W/m)
		Lat. (deg)	Long. (deg)				
80435	Acarigua	9.55	−69.23	226	2005–2009	2.328	15.126
80419	Barcelona	10.45	−64.68	7	2005–2008	2.492	11.998
80440	Barinas	8.62	−70.22	204	2005–2009	2.102	6.5758
80410	Barquisimeto	10.23	−69.32	613	2005–2008	3.704	38.185
80442	Calabozo	8.93	−67.42	101	2005–2007	2.243	10.631
80432	Carrizal	9.42	−60.92	835	2005, 2007–2008	2.093	11.22
80444	Ciudad Bolívar	8.15	−63.55	160	2005–2009	3.199	26.514
80492	Colon	8.03	−72.25	43	2007–2009	1.898	9.467
81435	Colonia Tovar*	10.42	−67.28	825	–	–	–
80403	Coro	11.42	−69.68	1435	2007–2009		104.02
80420	Cumana	10.45	−64.12	16	2005–2009		107.61
80437	El Vigía	8.63	−71.65	2	2005–2009		2.5621
80428	Guanare	9.08	−69.73	103	2005–2009		2.1372
80448	Guasdualito	7.23	−70.80	163	2006–2008–2009		6.1399
80423	Guiria	10.58	−62.30	130	2006–2009		37.517
80476	La Cañada	10.52	−71.65	13	2007–2009		20.48
80416	La Carlota*	10.50	−66.88	26	–	–	–
80439	Maiquetía	10.60	−66.98	63	2005–2009	1.258	11.54
80407	Maracaibo	10.23	−71.73	65	2006–2009	2.623	22.877
80413	Maracay	10.25	−67.65	436	2005–2009	1.874	4.9474
80435	Maturín	9.75	−63.18	68	2005–2009	2.925	20.503
80425	Mene Grande	9.78	−70.93	27	2005–2009	1.478	2.3458
80438	Mérida	8.60	−71.18	1479	2005–2009	2.474	9.389
80748	Palmichal	10.30	−68.23	1000	2007–2009	1.370	3.3584
80421	Porlamar	10.92	−63.97	24	2005–2007	5.137	106.01
80457	Puerto Ayacucho	5.60	−67.50	73	2006–2009	2.047	13.951
80447	San Antonio del Táchira	7.85	−72.45	377	2005–2009	2.795	43.131
80450	San Fernando	7.68	−67.42	47	2008–2009	2.101	9.025
80431	San Juan	9.92	−67.33	429	2006–2009	1.204	1.5194
80443	San Tomé	4.60	−61.12	262	2005–2009	1.171	46.923
80462	Santa Elena	9.55	−64.25	868	2006–2009	4.069	7.2799
80478	Santo Domingo	7.58	−72.07	328	2005–2009	1.940	1.8836
80478	Tembladór*	9.02	−62.62	30	–	–	–
80453	Tumeremo	7.30	−61.45	180	2005–2009	1.261	2.3121
80472	Valencia	10.17	−67.93	582	2005–2009	2.328	3.2214
80426	Valera	9.35	−70.62	430	2005–2008	2.492	2.4948
80434	Valle de la Pascua	9.22	−66.02	125	2005–2009	2.102	19.594

meteorological and Solar Energy (SSE) web portal supported by the NASA LaRC POWER Project [50]. The SSE dataset is a continuous and consistent 10-year meteorology dataset on a 1° latitude by 1° latitude equal-angle grid system. SSE winds are based on the Version 1 GEOS (GEOS-1) re-analysis dataset described in [51]. Although the SSE data within a particular grid cell are not necessarily representative of a particular microclimate, or point, within the cell, the data are considered to be the average over the entire area of the cell. For this reason, the SSE data set is not intended to replace quality ground measurement data. Its purpose is to fill the gap where ground measurements are missing, and to augment areas where ground measurements do exist.

Fig. 6 shows the geographical location of the $1^\circ \times 1^\circ$ wind data taken from the SSE re-analysis dataset.

3.1.3. Digital terrain data

The digital terrain data was used to provide information about terrain elevation, and it consists of a *Digital Elevation Model* (DEM) for terrain data which is used to divide the analysis region into individual grid cells, each one having its own unique elevation value. This paper uses the digital terrain data obtained from the *ASTER Global Digital Elevation Map* [52]. The ASTER elevation map provides updated DEMs for most of the world on 1° arc-second (30 m) grid of elevation postings.

Table 2
Details of the horizontal model domain and the interpolation grid.

Variable	Maximum	Minimum	Difference	Difference in km	Resolution [15 km]
Longitude	−57.120	−74.820	17.700	1917.294	128
Latitude	13.080	−0.550	13.630	1516.063	102

4. Results and discussion

This section presents the results and discussions of wind resource assessment in Venezuela using the methodology described in Section 2 and the input data presented in Section 3.

4.1. Model domain

This paper uses two main model domains: horizontal and vertical. For the horizontal domain, the standard spheroidal reference surface (the datum or reference ellipsoid) is used based on the *World*

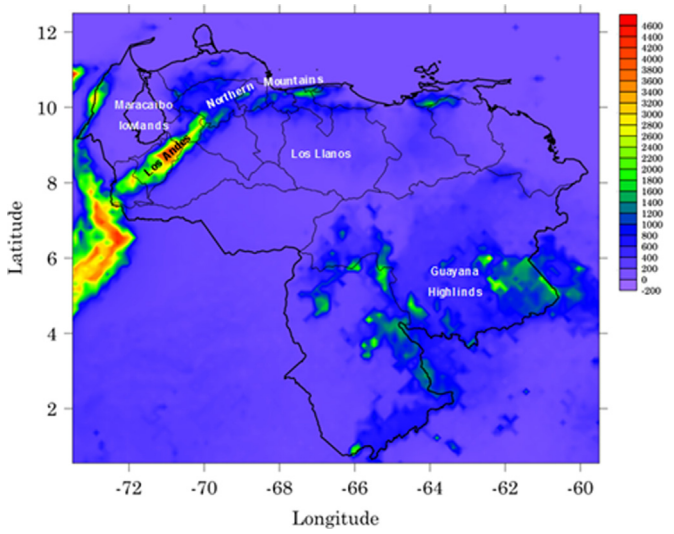

Fig. 7. Model domain and topography of Venezuela. Horizontal resolution is 15 km.

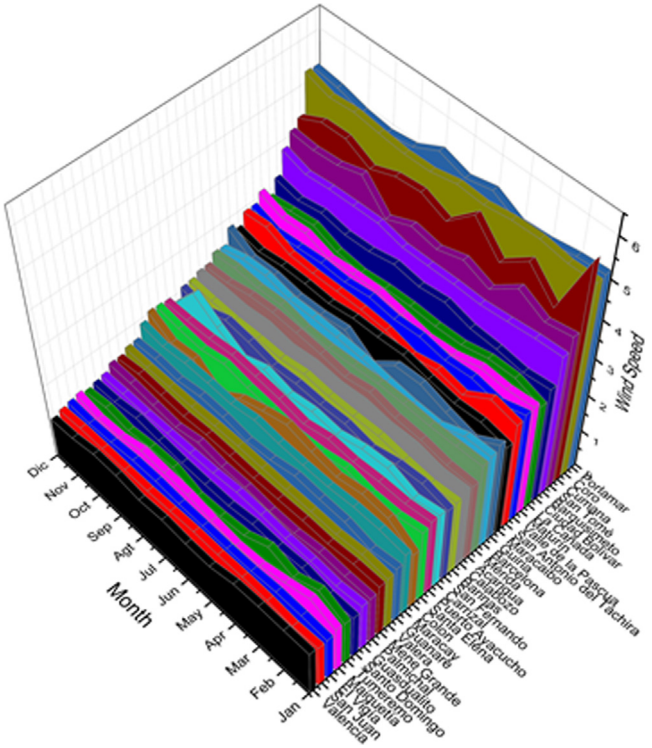

Fig. 8. Ground station monthly average wind speeds (m/s) at 50 mamsl.

Geodetic System (WGS). For the vertical domain, a *z*-system is used where *z* is the elevation above the sea level (Table 2).

4.2. Digital elevation model

As already mentioned, the Digital terrain data for the model domain was obtained from the *ASTER Global Digital Elevation Map* [52] and the original resolution of elevation model is 1 as grid i.e. it provides a resolution of approximately 30×30 m. For the wind resource extrapolation of the 3D terrain model, the original DEM dataset is re-gridded from the original $46{,}524 \times 60{,}157$ elevation data resolution using Kriging's spatial interpolation method to a finer resolution of 15 km (leading to 13,056 nodes).

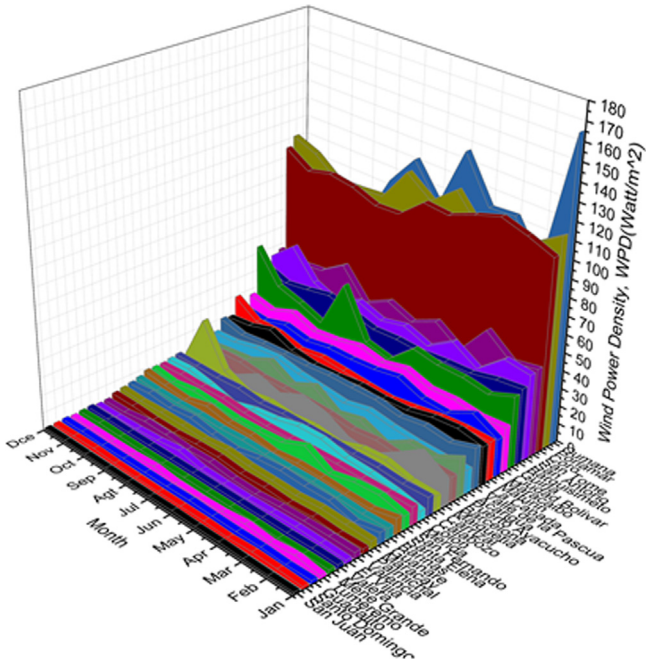

Fig. 9. Ground station monthly average wind power density (W/m^2) at 50 mamsl.

Table 3
Classes of wind power density at 50 m and 80 m.

Wind power class	Resource potential	Wind speed at 50 m (m/s)	Wind power density at 50 m (W/m^2)	Wind speed at 80 m (W/m^2)	Wind power density at 80 m (W/m^2)
1	Poor	<5.6	<200	<5.9	<251.3
2	Marginal	5.6–6.4	200–300	5.9–6.9	251.3–375
3	Fair	6.4–7.0	300–400	6.9–7.5	375.1–490
4	Good	7.0–7.5	400–500	7.5–8.1	490.8–604
5	Excellent	7.5–8.0	500–600	8.1–8.6	604–733
6	Outstanding	8.0–8.8	600–800	8.6–9.4	733–975
7	Superb	>8.8	800–2000	>9.4	>975

Fig. 7 shows the re-gridded DEM of Venezuela where four regions are identified: the *Maracaibo lowlands* in the northwest, the *northern mountains* extending in a broad east-west arc from the Colombian border along the Caribbean Sea, the wide *Orinoco plains* (Los Llanos) in central Venezuela, and the *Guyana highlands* in the southeast. It is worthwhile to highlight the terrain elevation characteristics for the "Los Andes" region, which includes a series of extremely high plateaus that are surmounted by even higher peaks. Pico Bolívar is the highest mountain in Los Andes at 4978 m (8°32′30″N, 71°2′45″W). A slope terrain dataset is calculated using the DEM in order to report the rise over run ($\Delta z/\Delta x$ and $\Delta z/\Delta y$). A very flat terrain with slopes between 0% to 10% are found in the Maracaibo lowlands and Los Llanos regions. However, Los Andes region exhibits a very complex orography with slopes as pronounced as 160%. Very high mountains, hills, escarpments and valleys located in Los Andes region are expected to give rise to significant local variations for the near-surface wind speed.

4.3. Wind resource characteristics in Venezuela

Fig. 6 shows the location of the monitoring sites belonging to the Venezuelan Air Force, and Table 1 provides a description of each site. Wind measurement equipment is installed at 37 sites. However this paper uses wind observations from 34 stations (due

to data availability). Datasets consist of wind speed and direction hourly ground observations at 10 mamsl from January 2005 to December 2009. The one-seventh-power law (see Section 2.5) is used to adjust the wind speed and power densities to a height of 50 m above ground. Wind data is processed to produce estimates of monthly average power densities and wind speeds as well as average wind direction. Annual average wind speed and power for the sites are included in Table 1.

Fig. 8 shows monthly average wind speeds at 50 mamsl for each ground stations ordered from yearly lower- (1.062 m/s) to higher-average (5.854 m/s). The higher wind speeds are found mainly at coastal site in northern Venezuela. Mean wind speeds over 4.00 m/s are found at San Tomé (80472), Cumaná (80427), Coro (80426), and Porlamar (80448). The southern locations of Venezuela exhibits very low wind speeds, and the lowest values (<1.25 m/s) are found at: Valencia (80472), San Juan (80462), and the El Vigía (80428). The average wind direction is mainly from the True North, especially true in northern locations. For South-eastern locations, wind directions are variable, but mainly point from 90° to 180° (measured clockwise from true North, 90°). Yearly average wind power density varies between 0.98 W/m^2 and 83.02 W/m^2, with a maximum monthly average of 122.92 W/m^2 in Cumaná (80427). The monthly average wind power density at 50 mamsl for each ground station is shown in Fig. 9. The higher values of wind power density 107.61, 106.01 and 104.02 W/m^2 are found in Cumaná (80427), Coro (80426), and Porlamar (80448), respectively. On the other hand, very low wind power densities (<2 W/m^2) are found in San Juan de Los Morros (80435) and Santo Domingo (80419).

4.4. Wind mapping and identification of resource areas

The calculation algorithm presented in Section 2 and the data discussed in Section 3 have been used to carry out wind the mapping process. The primary output of the mapping algorithm is a color-coded map showing equivalent mean wind speeds in units of m/s, and wind power map in units of W/m^2 for each individual grid cell. As indicated in Section 2.5, the one-seventh-power law was used to adjust the wind speed and power densities to a height of 50, 80 and 120 m above ground. The use of a height of 50 and 80 m is appropriate because, typically, utility-scale onshore wind turbines (greater than 1 MW) are installed at these heights or above, while small-scale wind turbines (approximately 10 kW) are installed on shorter towers. Higher wind turbines hub heights (up to 120 m) are typical for offshore applications.

The wind resource is typically expressed in *wind power classes* ranging from Class 1 (the lowest) to Class 7 (the highest). The wind power classification scheme of wind energy density is presented in Table 3.

Fig. 10 shows the results of the spatial interpolation of annual wind speeds de-compositioned in two components: (a) Zonal (v) and (b) Meridional (u). Wind speeds between -8 m/s and $+4$ m/s are found on both components. Zonal wind speed classified as *superb* are found on the northern coastal area of Venezuela and very low values are located in Amazonas state in southern Venezuela. The meridional component exhibits an average wind speed of approximately 1.12 m/s in the majority of the Venezuelan territory, peculiar high values (<-2.0 m/s) are located on the South–West of the Amazonas state near the border with Colombia and two more specific zones at Anzoátegui and Táchira states. Orographic correction is applied to wind the maps presented in Fig. 10 and results are shown in terms of the zonal and meridional components on Fig. 11.

Fig. 12 shows a convenient way of graphically presents changes on the main global statistical descriptors resulting from the orographic correction of the annual average wind speed (m/s) components. Whiskers have been included to indicate data variability outside the upper and lower quartiles. The main effect resulting from applying the orographic correction is a reduction on the standard deviation ($\Delta\sigma_v = -0.9280\%$, $\Delta\sigma_u = -0.4724\%$), a reduction in the mean value of the zonal component ($\Delta\overline{v} = -1.9216\%$) and a very small increase on the meridional component ($\Delta\overline{u} = +0.1620\%$).

Fig. 13 shows that the application of the orography correction leads to moderate changes in wind direction. The vectors in Fig. 13 illustrate direction and intensity changes to the velocity vector before and after applying the orographic correction. The prevailing winds coming from East/Northeast direction are predominantly the same across the majority of the orography in Venezuela. However, small changes on the wind direction are found after orographic correction. The digital elevation model has been included in Fig. 13 to show, however, a strong correlation between changes to wind direction due to terrain elevation. Small changes on wind direction ($<2°$) are mainly located at plain areas of Venezuela: Los Llanos. The complex topography of Los Andes with high slopes and heights up to 5000m produces, as expected, the more pronounced changes to the resulting

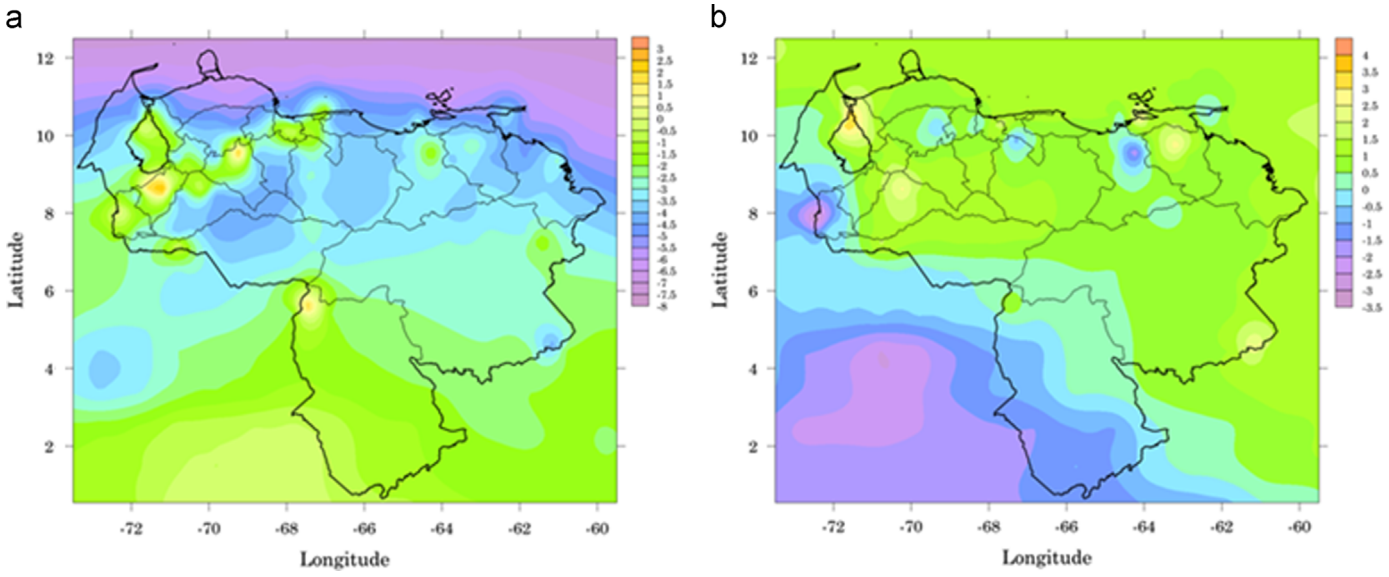

Fig. 10. Zonal (a) and meridional (b) velocity components resulting from the spatial interpolation of annual average wind speeds (m/s) at 50 mamsl.

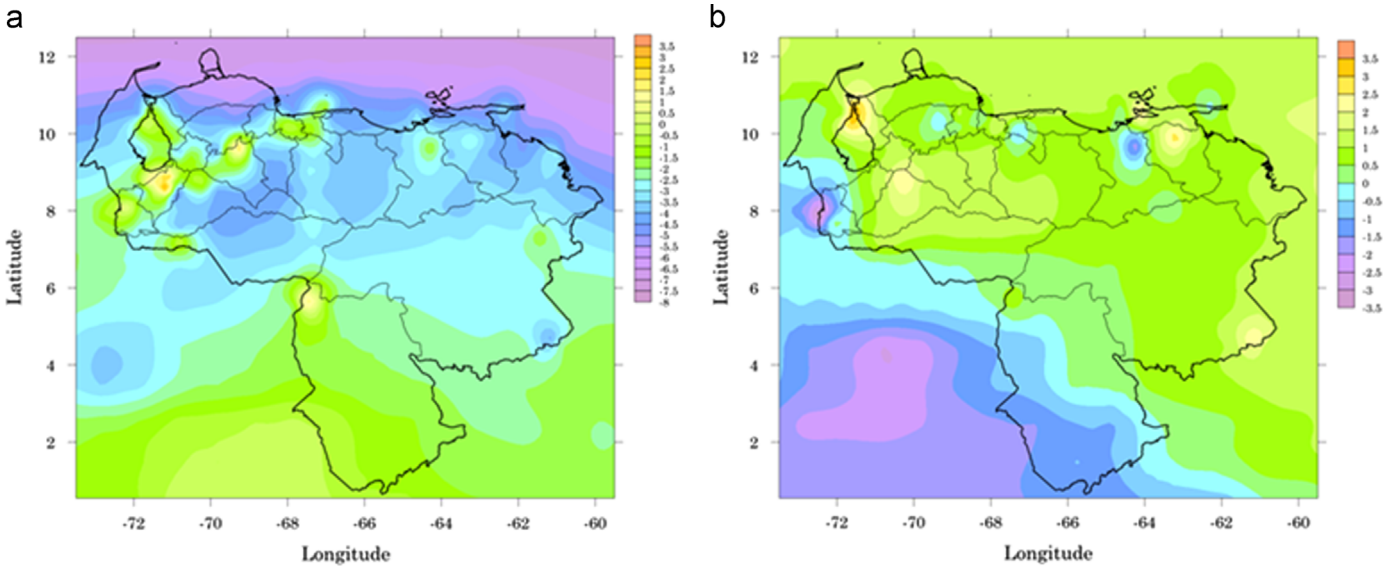

Fig. 11. Zonal (a) and meridional (b) velocity components resulting from the orographic correction of annual average wind speeds (m/s) at 50 mamsl.

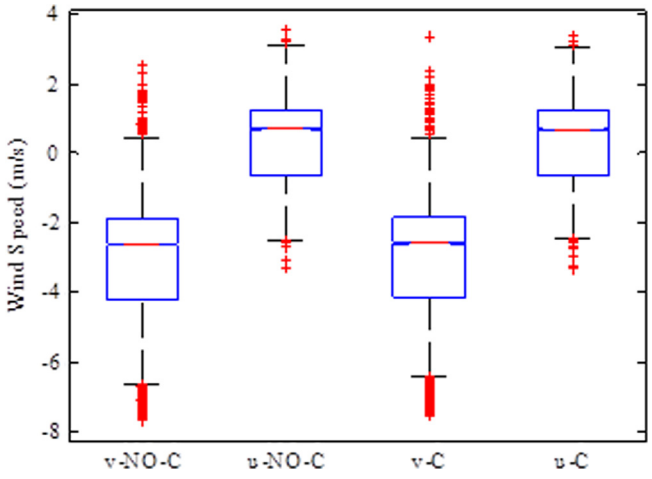

Fig. 12. Box plot of annual average wind speed components (v: zonal, u: meridional). NO-C—no orographic correction, C—orographic correction applied.

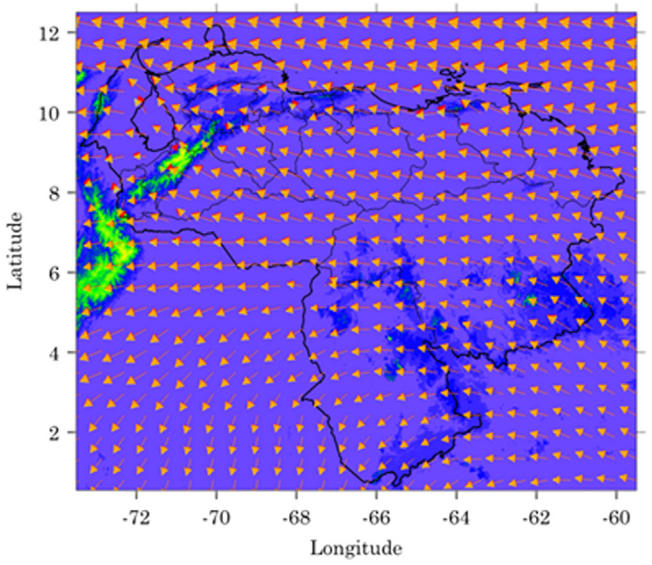

Fig. 13. Wind vectors indicating the direction and intensity of the wind before (red) and after orographic correction (yellow). (For interpretation of the references to color in this figure legend, the reader is referred to the web version of this article.)

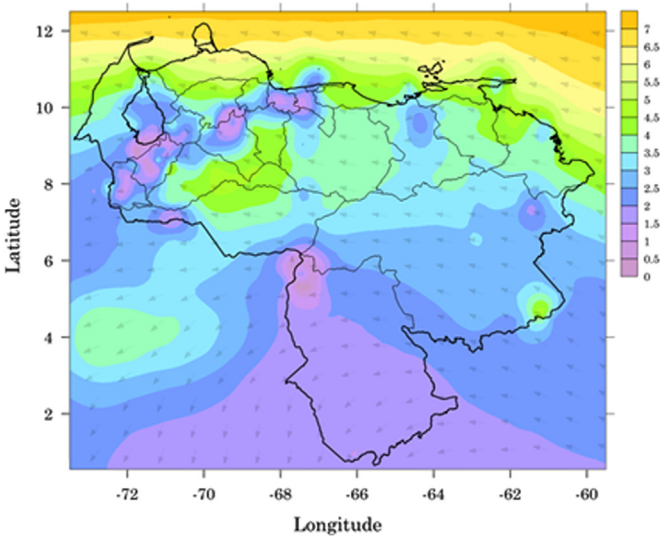

Fig. 14. Mean annual average wind speeds (m/s) at 50 mamsl in Venezuela.

wind direction ($<7^{\circ}$). Therefore, and due to the relative simplicity of the orography correction method used, the resulting wind speeds calculated within this region must be interpreted with caution.

Global patterns and distributions of wind speeds are preserved after applying the orographic correction in areas where there are no major changes in terrain slopes However, increases and reductions on wind speed components are evident in places like Los Andes where the spatial distribution of zonal wind speeds are more realistically correlated with the local topography. There are a couple areas where wind velocity is reduced as a consequence of the orography, zonal wind speeds in the Amazonas state near the Colombian border and the Anzoátegui state for the mediational component. A general reduction on the average speed of wind vector ($|\mathbf{v_H}|$) is linked to the smoothing effect originating from the flatness of the terrain and its vegetation roughness in the Maracaibo lowlands and Los Llanos regions ($\sim$92.7% of the Venezuelan surface).

The wind speed components when considering the orographic correction (Fig. 11) are combined in a single annual average wind speed map for Venezuela (Fig. 14). One of the effects of applying spatial interpolation is the generation of “bull’s-eyes” surrounding

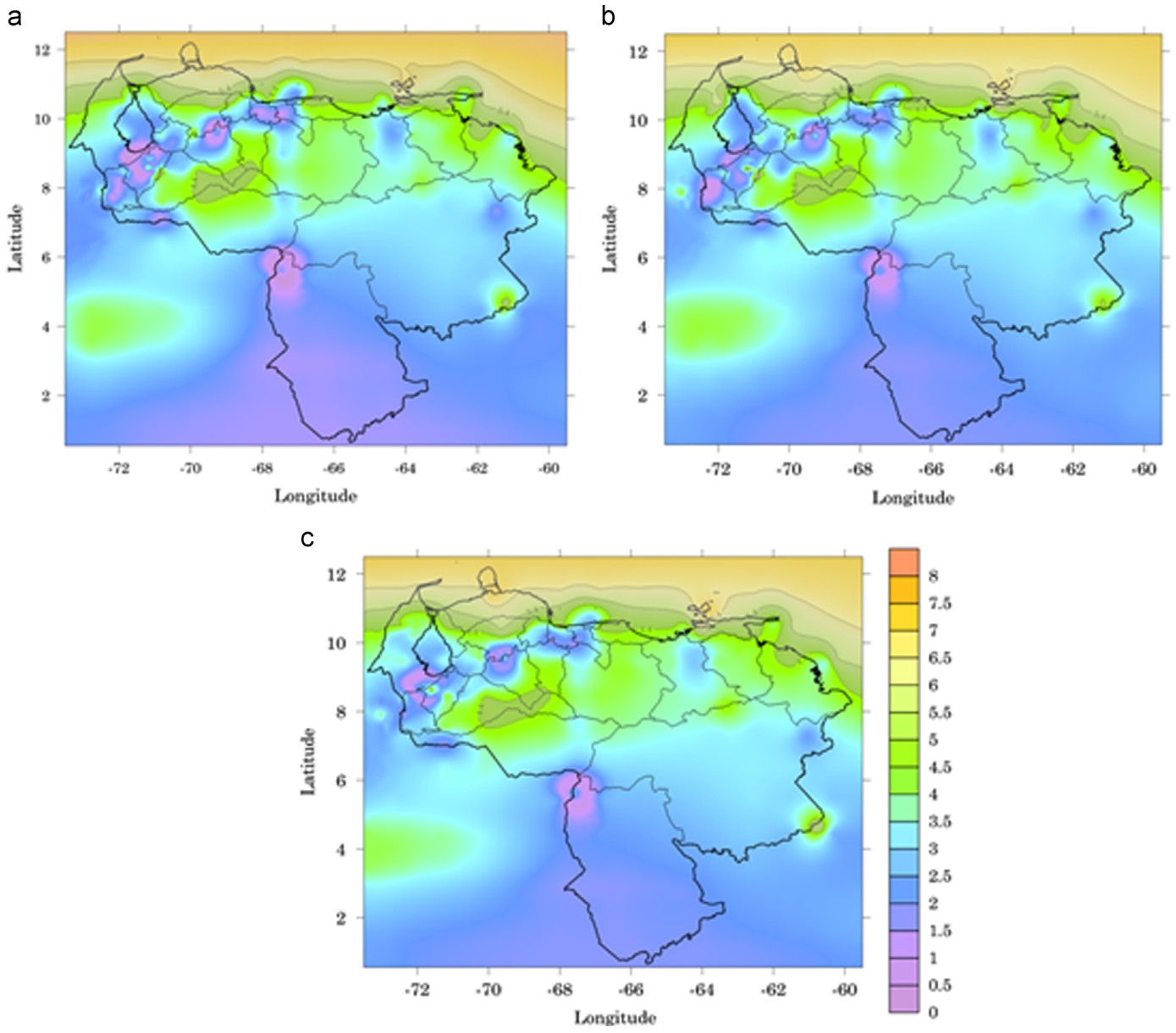

Fig. 15. Annual average wind speed (m/s) Map at 50, 80 and 120 mamsl.

the position of observations within the gridded area. However, the use of the advanced geo-statistical Kriging method and the orographic correction provided a better estimate of wind resource in the investigated area from a dispersed set of meteorological stations.

Fig. 14 shows results of the predicted Venezuelan wind speed map at 50 mamsl, and shows that the velocity inside the Venezuelan territory varies from 0.216 to 6.740 m/s. Moderate to low deviations of individual velocities from the mean value are found in the wind map, the standard deviation of the horizontal component of the wind speed is 1.474 m/s which represents a moderate variability between regions in Venezuela.

The results shows that a potential onshore area of 13,298.7 km^2 is available for wind power generation using utility-scale wind turbines or smaller turbines. Wind resources within the class 1 band which are suitable for utility-scale applications are found in 85.96% (11,432.2 km^2) of the Venezuelan territory and class 2 wind resources have been predicted for an area of 1866,48 km^2 (representing 14% of the Venezuelan territory). Additionally, it must be noticed that superb wind resource potential were not predicted in the territory, however, there are several offshore areas where the wind speed is over 7.0 m/s (Fig. 14).

The wind resource in Venezuela is strongly dependent on elevation and proximity to the coastline, as it can be seen in Fig. 14. In general, the wind resource is best on hilltops, ridge crests, and coastal locations which have excellent exposure to the prevailing winds that blow from the East. The extreme North-eastern and North-western regions of the country are estimated to have the greatest number of areas with good-to-excellent wind resources for utility-scale applications due to the presence of upper-air winds and ocean winds which are greatest within these regions.

Wind speed maps at three different heights are presented on Fig. 15 on which shadows are used to identify areas where the wind speed is greater than 4.4 m/s. The majority of the coastline areas in Venezuela exhibit moderate wind speeds (approximately 4 m/s): Zulia, Falcon and Sucre State, Margarita Island, and a small part of the Miranda State coastline. The northern part of the Lara state, almost all of the Urdaneta district, exhibits relatively high horizontal wind speeds. There is a small part in Los Llanos region (Barinas state and a small portion in the Cojedes and Apure state)

Table 4
Available surface (km^2) at 50, 80 and 100 mamsl classified for various wind speed intervals.

Wind speed at	< 5.6	5.6–6.4	6.4–7.0	7.0–7.5
50 m	890,780.8 (97.20)	12,832.0 (1.40)	3499.3 (0.38)	0
80 m	884,481.4 (96.51)	15,165.2 (1.62)	5132.8 (0.76)	0
120 m	888,214.3 (96.62)	12,132.1 (1.32)	6999.3 (0.56)	1166.5 (0.13)

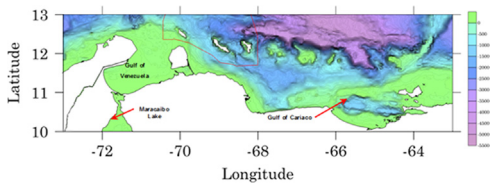

Fig. 16. Venezuelan seabed map. The bathymetry is represented down to 500 average wind speed km in the sea and the red line identifies a limit for an exclusively economical area.

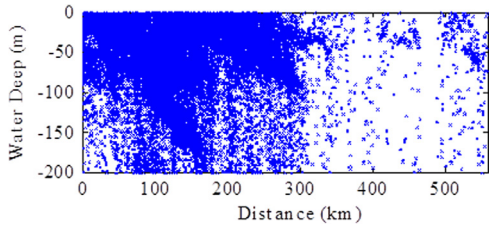

Fig. 17. Water depth for the Venezuelan littoral versus distance measured from the shore.

Table 5
Offshore area available per type of aggregated land and cover class (km^2) at 80 m.

Foundation type	Water deep (m)	Total area available (km^2)	Total area $V_w < 7.0$ m/s	Total area $V_w > 7.0$ m/s
Shallow water	0–30	45,722.28	45,127.89	594.38
Transitional	30–50	21,316.10	16,285.50	5030.6
Deep water	50–200	55,960.46	51,175.84	4784.61

which exhibit moderate wind speeds (approximately 4 m/s). Wind speeds for the southern states in Venezuela have very low wind speeds where the wind speed is lower than 4.4 m/s, which is insufficient for utility-scale applications, however, small-scale off-grid applications might be possible and deserves further study.

The mean horizontal wind speed in Venezuela exhibits increases as the height above ground level increases, leading to an increase in surface area where high wind speeds are available. Table 4 shows the available surface area classified using representative wind speed intervals at several heights. Additionally, percentage figures expressed in relation to the total onshore surface of Venezuela are given in parentheses in order to provide a reference datum. As the height increases, the surface proportion covered by high horizontal wind speeds is also shown to increase. The available surface with wind speeds in the range 6.7–7.0 m/s increases from 3499.3 km^2 to 5132.8 km^2 when the reference height is changed from 50 to 80 m. A special mention is deserved to the changes on the surface area in the Falcon state covered by high winds. At 50 m, 87% of the Paraguaná Peninsula offers winds with moderate-high speeds (6.4–7.0 m/s), but this area is increased to 100% and part of onshore territory of the Falcon state (Zamora and Colina districts) are covered with the same wind speed at a height of 80 m. Wind speeds greater than 7.0 m/s are found at the north of the peninsula of Paraguaná at 120 m.

Margarita Island is confirmed as a location with high wind speeds for all heights evaluated in this paper, the entire surface offers wind speeds above 6.0 m/s at 50 mamsl. Winds speeds above 6.5 m/s at 120 m are found in more than 73% of Margarita Island and the East shores and Cubagua and Coche Islands, as consequence this area is highlighted for future assessment in order to provide more information for potential utility-scale onshore and offshore applications and deserves to be further investigated.

4.4.1. *Short discussion: Offshore wind resources*

Wind speeds for offshore applications at Venezuelan coast looks really attractive. The Venezuelan coastline is 2718 km long and provides privileged access to an important area of Caribbean Sea. The *United Nations Convention on the Law of the Sea* (UNCLOS) defines several maritime claims: *territorial sea* (12 nm), *contiguous zone* (15 nm), *exclusive economic zone—EEZ* (200 nm) and a continental shelf with a 200 m depth, or to the depth of exploitation. When selecting a location for an offshore wind farm, the water depth and seafloor characteristics need to be evaluated.

Fig. 16 shows a seabed map including a main part of the Venezuelan coast, until 500 km and the EEZ which represents a total surface area of 471,507 km^2. Seafloor characteristics determine how difficult it would be to construct a wind farm at that location. Water depth has a strong influence on the total cost of a wind turbine installation due to the cost of building appropriate support structures. Offshore wind turbines are installed using a variety of foundation structures depending on the depth of the water: *Shallow water*, *Medium water,* and *Deep water* (50–200 m).

The deepest point at the seabed of the Venezuelan EEZ is $z = -5227.4$ m which is slightly higher than the deepest point in the Caribbean zone (-6946 m), but the average depth in this zone is around -2400 m which is beyond the acceptable water depth for offshore wind power applications. Water depths between 0 and 200 m, suitable for offshore wind power, is found in several areas where the wind resource has been identified excellent (Fig. 15).

The Gulf of Venezuela, Falcon and Carabobo states have depths of approximately 200 m for distances up to 125 km from the shore. Locations like Aragua and Vargas exhibit a seabed with high slopes, where within a few kilometres the water depth reaches more than 2 km deep. Specially, the Gulf of Cariaco on the north central coast of Venezuela which separates (~1400 m depth) Margarita Island and the states of Anzoátegui and Sucre. Details of the bathymetry of Venezuelan littoral zone are shown on Fig. 17.

A preliminary water depth assessment on the Venezuelan EEZ indicate that 26.08% of the seabed surface is suitable to for offshore wind power applications when considering actual trends to enable full exploitation of offshore wind resources. Results shown on Table 5 indicate the seabed conditions for medium depth water or transitional foundations are available on 17.3% of the total surface usable for wind power, however, the floating platform concept available for deep waters can be used in 45% of the Venezuelan coatline.

Wind mapping results show a sharp increase in yearly average wind speeds as the distance from shore increases. Wind speeds of 7.0 m/s and above are found in all Venezuela EEZ. However, water depth increases as distance from shore increases. The distance a wind project is from shore determines a project's viability because the distance affects the potential development cost due to considerations such as the length of underwater cables needed to connect the offshore wind project to the land-based electricity distribution facilities.

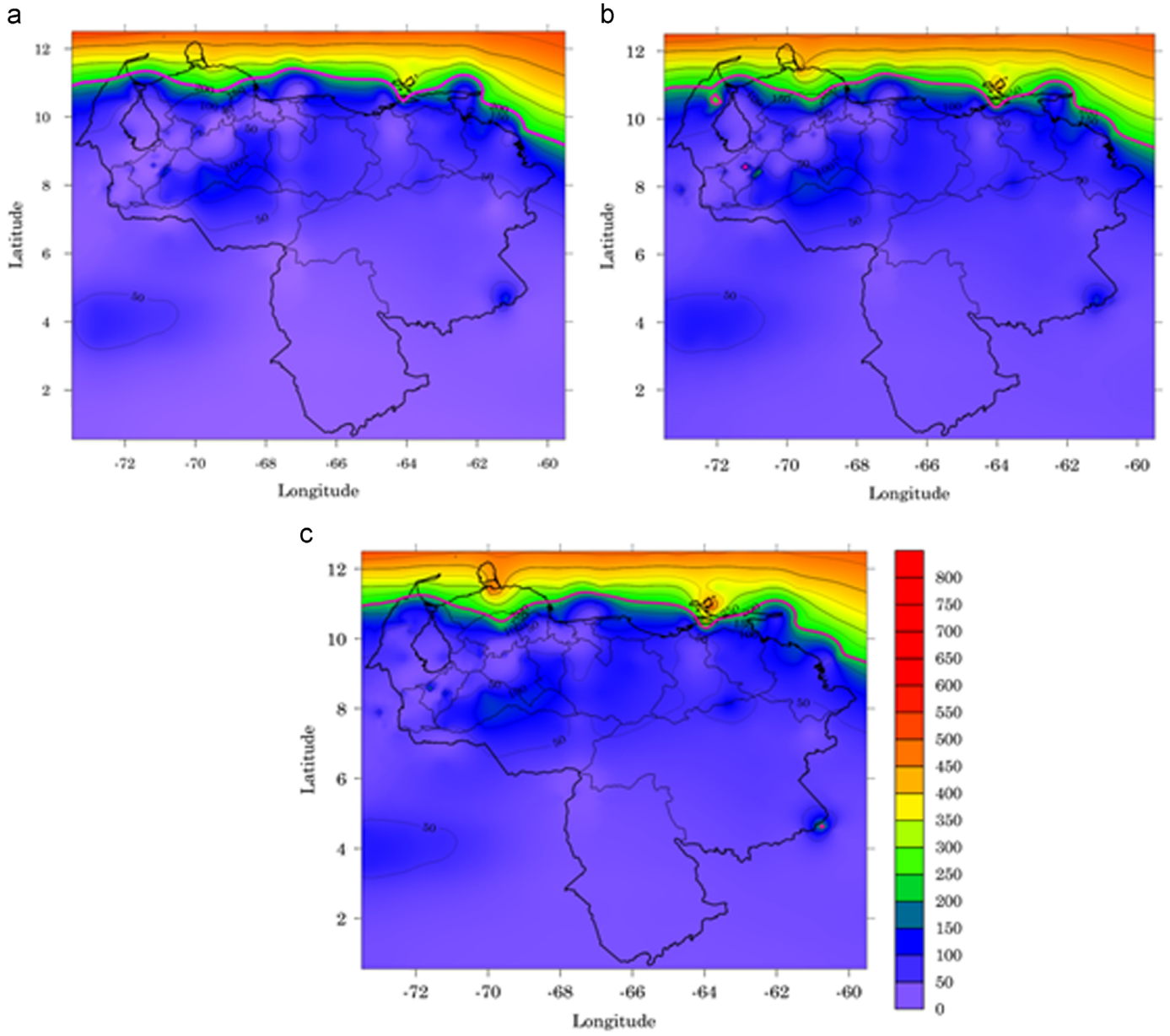

Fig. 18. Annual average wind power density (m/s) map at 50, 80 and 120 mamsl.

Table 6
Available surface (km^2) classified per wind speed available at 50, 80 and 100 mamsl.

Hub-height	Wind power density (W/m^2)			
	< 200	200–400	400–500	500–600
50 m	887,747.7 (96.86)	14,698.5 (1.60)	235.23 (0.025)	0 (0.0)
80 m	880,281.8 (96.05)	18,664.868 (2.03)	115.1 (0.012)	933.243 (0.10)
120 m	881,448.3 (96.18)	15,865.137 (1.73)	87.01 (0.009)	2099.798 (0.22)

The Venezuelan seabed is relatively flat in areas like the Venezuelan Gulf and the west of the Falcon State which would allow using shallow water and transition foundations for larger distances at the east coastal area of Venezuela. The available seabed surface for the use of offshore wind turbine foundations actually available (< 200 m) is evaluated, this assessment considers only wind speeds of 7.0 m/s or greater to establish suitable areas for offshore wind power exploitation (the results are shown in column four and five of Table 5). The available areas for offshore wind power exploitation in the Venezuelan cost using foundations down to a depth of 50 m represent 54.4% of the use of wind speed above 7.0 m/s. More than half (45.96%) of the surface available which exhibit a wind resource with speeds greater than 7.0 m/s requires the use of deep water foundations. This simple and preliminary assessment of wind speed at the Venezuelan littoral demonstrates there are enough wind resources for utility

Table 7
Assumptions used for calculating the wind energy potential per unit of windy land area.

Hub-height	80 m			120 m		
Power density (W/m^2)	Average power captured (MW/km^2)	Average power output (MW/km^2)	Annual energy production (kW h/km^2/yr)	Average power captured (MW/km^2)	Average power output (MW/km^2)	Annual energy production (GW h/km^2/yr)
200	3.141	0.5908	5.122	9.622	1.809	1.5692
400	6.282	1.1779	10.212	19.244	3.608	3.1284
500	7.853	1.470	12.745	24.055	4.503	3.9043
600	9.423	1.729	14.992	28.867	5.297	4.5926

Table 8
Wind electric potential in Venezuela.

Hub-height	80 m		120 m	
Power density (W/m^2)	Total capacity installed (MW)	Total power (GW h/year)	Total capacity installed (MW)	Total power (GW h/year)
200–400	21,986.63	20,396.78	57,247.61	53,604.37
400–500	345.81	155.51	391.83	35.67
500–600	1,613.82	1,455.15	11,122.88	1,012.57
Total	23,946.26	22,007.43	68,762.32	54,652.61

production which are located in areas that allow the use of support structures that are commercially available (up to 200 m water deep).

4.5. Wind electric potential

The wind electric potential is an estimated forecast of the amount of energy that the winds at a given site or in a given area could provide if a wind energy facility were established.

Several factors determine the amount of land area suitable for wind energy development within a particular grid cell in a region of high wind energy potential. The important factors to consider include (i) the percentage of land exposed to the wind resource, (ii) land-use, and (iii) any environmental restrictions. The wind electric potential per grid cell is calculated in this paper using the available windy land area and the wind power classification assigned to each cell. The amount of potential electricity that can be generated is dependent on several factors, including the spacing between wind turbines, the assumed efficiency of the machines, the turbine hub height, and the estimated energy losses caused by wind turbine wakes, blade soiling, etc. [53].

The wind energy resource map of Venezuela shows that areas potentially suitable for wind energy applications are dispersed throughout the northern coastal area of Venezuela, and offshore wind power looks attractive for utility-scale exploitation. Estimates of the wind resources in this map are expressed in wind power densities ranging from 200 to 600 W/m^2 for onshore wind power applications, and up to 800 W/m^2 for offshore applications.

In this paper, areas designated with power densities between 200 W/m^2 or greater are suitable for advanced wind turbine technology for utility-scale utilization and wind power densities of 200 W/m^2 and below areas that can be used for other applications.

Fig. 18 shows the Venezuelan wind resource map for three different hub heights (50, 80 and 120 mamsl), and a red line is included in each map to separate areas considered high/low power density (>200 W/m^2).

The main areas of the coastline in Venezuela have very high wind power density (>200 W/m^2): Zulia, Falcon and Sucre States, and Margarita Island. Also, very high values are found in Lara state. There is small area within the Guayana Highland which exhibits moderate wind power densities (>200 W/m^2 at 80 and 120 m) and requires further evaluations.

The wind power density is very low at the southern states of Venezuela where the wind resource is insufficient for utility-scale usage but small-scale off-grid application might be evaluated, however, such evaluation is beyond the scope of this paper.

Table 6 shows the available surface in Venezuela which is classified per wind power density at several heights and percentage figures expressed in proportion of the total onshore surface of Venezuela are given in parentheses for reference. As the height increases, the surface proportion covered by high wind power density also increases.

The available surface with a wind power density between 200 and 400 W/m^2 increases from 14,698.5 km^2 to 18,664.8 km^2 when the height increases from 50 to 80 m. Special mention deserves the changes on the surface area covered with high wind power density in the Falcon state. At 50 m, 100% of the Paraguaná Peninsula, 82.3% of Falcon state and 11% of Lara state offer a wind power density above 300 m/s, but this area is increased to 93.4% and part of onshore territory of Falcon state (Zamora and Colina districts) are covered with the same wind speed at a height of 80 m. Wind power density up to 403.5 W/m^2 are found at the northern part of the peninsula of Paraguaná at 120 m.

In this paper, several assumptions are used to calculate the *wind energy potential* per unit of windy land area. The main assumptions and methods for converting the wind resource to wind energy potential are based in a modified version of those presented in [54]. Wind turbine's hub high is assumed to be 80 m 120 m and the wind turbines are combined in a wind farm with a regular array. Future technological development of wind energy are assumed based on [55], considering an availability of 98%. A $10D \times 5D$ spacing is used for the wind turbine array, where D is the wind turbine diameter. These assumptions help define the main characteristics to predict the wind electric potential per grid cell (details are presented in Table 7).

Each square kilometre on the map has an annual average wind power density (in W/m^2) at a height of 80 m and 120 m. An equation has been developed to compute the total net annual energy delivery for each square kilometre with an annual average

wind power density of 200 W/m^2 or greater. If the wind power density was less than 200 W/m^2, the net energy potential is not considered for further calculation in this paper because these grid cells have insufficient wind potential for the economic development of utility-scale wind energy.

Although the areas with lower wind resources (100–200 W/m^2) are not economical for utility-scale wind, they have the potential for the isolated use of small wind turbines for rural electrification projects. Under those considerations, only grid cells with an annual average wind power density of 200 W/m^2 or greater are considered.

The wind resource levels shown in Table 7 are consistent with those on the wind resource maps for the Venezuelan territory (Figs. 13 and 17). The numbers in the table represent total net wind-energy potential, and they have not been reduced by factors such as land-use exclusions. The estimated net energy has been reduced by 15–20% to account for expected losses due to down-time, wake effects, and other factors.

Results from this work demonstrate that there are approximately 15,000 km^2 of land-area with wind resource potential for utility-scale applications at 80 m. The proportion of windy lands and potential wind capacity in each wind power category is listed in Table 8. This windy land represents less than 1.98% of the total land area (916,445 km^2) of the Venezuelan territory. Despite using conservative assumptions (7 MW per km^2), this windy land could support more than 23,000 MW of potential installed capacity, and could potentially deliver over 53 billion kilowatt-hours (kW h) per year. Considering only the areas where wind power density is above 200 W/m^2, there are 4 states (Sucre, Lara, Nueva Esparta and Anzoátegui) in Venezuela with at least 1500 MW of wind potential and main areas of the Falcon state and Venezuelan Guajira (Zulia state) with at least 3000 MW of wind potential.

However, additional studies are required in order to more accurately assess the wind electrical potential, to include factors such as the existing transmission grid and accessibility. Assessment of offshore wind electrical potential requires further investigation.

The additional exploration of wind electrical potential at 120 m indicates that the estimated total windy land area increases to more than 5400 km^2, or slightly more than 2.15% of the total land area of Venezuela. This windy land could support more than 65,000 MW of potential installed capacity and potentially deliver over 54 billion kW h per year.

5. Conclusions

Mesoscale modelling for wind energy resource mapping is a well-established method which has two important limitations: its input data requirements and its computational cost. This paper presented a step forward for rapid mesocale wind modelling. The calculation method uses a simple geo-statistical Kriging method to interpolate horizontal wind speed and then an orographic correction is applied in order to correct horizontal wind speeds due to changes in terrain elevation. The resultant method is a computationally economical alternative to mesoscale modelling and includes exploratory statistical analysis of the wind data which has been applied in order to provide a wind resource assessment in Venezuela. Hourly observations of wind speed and direction from 34 anemometer masts belonging to the meteorological network of the Venezuelan Air Force (MSVAF) recorded during the period 2005–2009 have been analysed in order to define a statistical model of wind resources for the entire Venezuelan territory. Simulations results include color-coded maps of the equivalent mean wind speeds and a wind power map have been created for heights of 50, 80 and 120 m above ground at a horizontal resolution of 15 × 15 km.

The main effect of applying the orographic correction is a reduction on the standard deviation, a reduction in the mean value of the zonal component, and a very small increase on the meridional wind velocity component. The prevailing winds coming from East/Northeast direction are predominantly the same across almost all the orography in Venezuela. Small changes in wind direction are mainly found within the plain areas of Venezuela (Los Llanos) and the complex topography of Los Andes produces slightly more pronounced changes.

The results obtained in the performed analysis show average wind speeds between 6.835 m/s onshore and 8.573 m/s for off-shore locations. The highest wind speeds are found in the northern area of Venezuela, mainly in coastal sites. High mean wind speeds are also found in Zulia, Falcon, Lara, Anzoátegui, Sucre and Nueva Esparta. The southern locations of Venezuela exhibit very low wind speeds, where the lowest values are found in Valencia and San Juan de los Morros. Results also show that the best wind energy resources are located in the coastal northern area of Venezuela with an extraordinary potential for offshore applications.

There is approximately 15,000 km^2 of land with wind resource potential for utility-scale applications at 80 m and additional exploration of wind electrical potential at 120 m indicates that the estimated total windy land area increases to slightly more than 2.15% of the total land area of Venezuela. Using conservative assumptions for estimating windy lands, the evaluation presented in this work indicates that they could support more than 65,000 MW of potential installed capacity, and deliver over 54 billion kilowatt-hours (kW h) per year. Wind energy resources for commercial use (utility-scale) is possible in Venezuela within a reasonable area of northern Venezuela and there are also excellent conditions for wind power production for micro-scale applications, on- and off-grid.

References

[1] FM Gonzalez-Longatt. Evaluation of reactive power compensations for the phase I of Paraguaná wind based on system voltages. In: Presented at the 39th annual conference of the IEEE Industrial Electronics Society (IECON 2013), Vienna, Austria; 2013.

[2] F Gonzalez-Longatt. Systemic impact caused by the integration of La Guajira wind farm. In: Presented at the 39th annual conference of the IEEE Industrial Electronics Society (IECON 2013), Vienna, Austria, 2013.

[3] F González-Longatt, J Méndez, R Villasana. Preliminary evaluation of wind energy utilization on Margarita Island, Venezuela. In: Sixth international workshop on large-scale of integration of wind power and transmission networks for offshore wind farms, Delft, The Netherlands; 2006.

[4] F González-Longatt, J Méndez, R Villasana, C Peraza. Wind energy resource evaluation on Venezuela: Part I. In: Presented at the Nordic wind power conference NWPC 2006, Espoo, Finland; 2006.

[5] FM Gonzalez-Longatt. Systemic impact caused by the integration of La Guajira wind farm. In: Presented at the 39th annual conference of the IEEE Industrial Electronics Society (IECON 2013), Vienna, Austria; 2013.

[6] VMContreras, VV Elistratov. Evaluación técnica del recurso eólico en Venezuela. In: Presented at the 12th world wind energy conference & renewable energy exhibition WWEC2013, Havana, Cuba; 2013.

[7] LnEG. Avaliação do Recurso Solar e Eólico para a Venezuela. Available: ⟨http://www.lneg.pt/iedt/projectos/451/⟩; 2014.

[8] Brower M. Wind resource assessment: a practical guide to developing a wind project. Hoboken, NJ: John Wiley & Sons, Inc.; 2012.

[9] Yaniktepe B, Koroglu T, Savrun M. Investigation of wind characteristics and wind energy potential in Osmaniye, Turkey. Renewable Sustainable Energy Rev 2013;21:703–11.

[10] Mostafaeipour A, Sedaghat A, Dehghan-Niri A, Kalantar V. Wind energy feasibility study for city of Shahrbabak in Iran. Renewable Sustainable Energy Rev 2011;15:2545–56.

[11] Ahmed Shata A, Hanitsch R. Evaluation of wind energy potential and electricity generation on the coast of Mediterranean Sea in Egypt. Renewable Energy 2006;31:1183–202.

[12] Aman M, Jasmon G, Ghufran A, Bakar A, Mokhlis H. Investigating possible wind energy potential to meet the power shortage in Karachi. Renewable Sustainable Energy Rev 2013;18:528–42.

[13] Mpholo M, Mathaba T, Letuma M. Wind profile assessment at Masitise and Sani in Lesotho for potential off-grid electricity generation. Energy Convers Manage 2012;53:118–27.

[14] Ozgener L. Investigation of wind energy potential of Muradiye in Manisa, Turkey. Renewable Sustainable Energy Rev 2010;14:3232–6.

[15] Janajreh I, Su L, Alan F. Wind energy assessment: Masdar City case study. Renewable Energy 2013;52:8–15.
[16] Wu J, Wang J, Chi D. Wind energy potential assessment for the site of Inner Mongolia in China. Renewable Sustainable Energy Rev 2013;21:215–28.
[17] F Ben Amar, M Elamouri, R Dhifaoui. Energy assessment of the first wind farm section of Sidi Daoud, ed: Tunisia; 2008.
[18] Youm I, Sarr J, Sall M, Ndiaye A, Kane M. Analysis of wind data and wind energy potential along the northern coast of Senegal. Rev Energ Ren 2005;8:95–108.
[19] Tchinda R, Kaptouom E. Wind energy in Adamaoua and North Cameroon provinces. Energy Convers Manage 2003;44:845–57.
[20] Himri Y, Himri S, Stambouli A Boudghene. Assessing the wind energy potential projects in Algeria. Renewable Sustainable Energy Rev 2009;13:2187–91.
[21] Himri Y, Rehman S, Agus Setiawan A, Himri S. Wind energy for rural areas of Algeria. Renewable Sustainable Energy Rev 2012;16:2381–5.
[22] Hernández-Escobedo Q, Saldaña-Flores R, Rodríguez-García E, Manzano-Agugliaro F. Wind energy resource in Northern Mexico. Renewable Sustainable Energy Rev 2014;32:890–914.
[23] Palomino I, Martin F. A simple method for spatial interpolation of the wind in complex terrain. J Appl Meteorol 1995;34:1678–93.
[24] Apaydin H, Sonmez FK, Yildirim YE. Spatial interpolation techniques for climate data in the GAP region in Turkey. Clim Res 2004;28:31–40.
[25] Carrera-Hernández J, Gaskin S. Spatio temporal analysis of daily precipitation and temperature in the Basin of Mexico. J Hydrol 2007;336:231–49.
[26] Ninyerola M, Pons X, Roure JM. Monthly precipitation mapping of the Iberian Peninsula using spatial interpolation tools implemented in a Geographic Information System. Theor Appl Climatol 2007;89:195–209.
[27] Z Zlatev, SE Middleton, G Veres. Ordinary kriging for on-demand average wind interpolation of in-situ wind sensor data, presented at the EWEC 2009; 2009.
[28] Luo W, Taylor MC, Parker SR. A comparison of spatial interpolation methods to estimate continuous wind speed surfaces using irregularly distributed data from England and Wales. Int J Climatol 2008;28:947–59.
[29] K Yonga, M Ibrahima, M Ismaila, A Albania, A Muzathikb. Wind mapping in malaysia using inverse distance weighted method.
[30] Cellura M, Cirrincione G, Marvuglia A, Miraoui A. Wind speed spatial estimation for energy planning in Sicily: introduction and statistical analysis. Renewable Energy 2008;33:1237–50.
[31] Xydis G, Koroneos C, Loizidou M. Exergy analysis in a wind speed prognostic model as a wind farm sitting selection tool: a case study in Southern Greece. Appl Energy 2009;86:2411–20.
[32] Liao S, Liu K, Li Z. Estimation of grid based spatial distribution of wind energy resource in China. Geo-Inf Sci 2008;5:002.
[33] Hossain J, Sinha V, Kishore V. A GIS based assessment of potential for windfarms in India. Renewable Energy 2011;36:3257–67.
[34] S Ali, A Shaban, AK Resen. Integrating WAsP and GIS tools for establishing best positions for wind turbines in South Iraq.
[35] Sathyajith M. Wind energy: fundamentals, resource analysis and economics. New York, NY: Springer-Verlag Inc.; 2006.
[36] M Brower. Validation of the WindMap Program and Development of Meso-Map. In: AWEA's WindPower conference, Washington, DC; 1979.
[37] Matheron G. Les variables régionalisées et leur estimation: une application de la théorie des fonctions aléatoires aux sciences de la nature. Paris: Masson et Cie; 1965.
[38] Oliver MA, Webster R. A tutorial guide to geostatistics: computing and modelling variograms and kriging. CATENA 2014;113:56–69 2//.
[39] Cressie NAC. Statistics for spatial data. New York, NY: John Wiley and Sons, Inc.; 1991.
[40] Journel AG, Huijbregts CJ. Mining geostatistics. London, New York, San Francisco: Academic Press; 1978.
[41] Song MX, Chen K, He ZY, Zhang X. Wind resource assessment on complex terrain based on observations of a single anemometer. J Wind Eng Ind Aerodyn 2014;125:22–9 2//.
[42] Stangroom P. CFD modelling of wind flow over terrain. UK: Doctor of Philosophy, University of Nottingham; 2004.
[43] Saavedra-Moreno B, Salcedo-Sanz S, Casanova-Mateo C, Portilla-Figueras JA, Prieto L. Heuristic correction of wind speed mesoscale models simulations for wind farms prospecting and micrositing. J Wind Eng Ind Aerodyn 2014;130:1–15 7//.
[44] JF Ruiz, HJ Zapata. Algoritmo Usado para Estimar Energia Eolica en Colombia. Available: ⟨http://koha.ideam.gov.co/cgi-bin/koha/opac-detail.pl?biblionumber=39518&shelfbrowse_itemnumber=38655⟩; 2010.
[45] Jackson PS, Hunt JCR. Turbulent wind flow over a low hill. Q J R Meteorol Soc 1975;101:929–55.
[46] Belcher SE, Hunt JCR. Turbulent flow over hills and waves. Annu Rev Fluid Mech 1998;30:507–38.
[47] EH Lysen. Introduction to wind energy: basic and advanced introduction to wind energy with emphasis on water pumping windmills. Available: ⟨http://docs.watsan.net/Downloaded_Files/PDF/Lysen-1982-Introduction.pdf⟩; 1982.
[48] Inameh. Instituto Nacional de Meteorología e Hidrología informa—Inameh. Available: ⟨http://www.inameh.gob.ve/⟩; 2012 (06 Feb 2014).
[49] FAV. Servicio de Meteorologia de la Aviacion. Available: ⟨www.meteorologia.mil.ve/⟩; 2012 (1 Mar 2014).
[50] NASA. NASA Langley research center atmospheric science data center surface meteorological and solar energy (SSE) web portal. Available: ⟨https://eosweb.larc.nasa.gov/sse/⟩; 2010.
[51] LL Takacs, A Molod, T Wang. Volume 1: Documentation of the Goddard Earth Observing System (GEOS) general circulation model—version 1, NASA Technical Memorandum 104606, NASA, USA; 1994.
[52] ASTER. ASTER global digital elevation map. Available: ⟨http://asterweb.jpl.nasa.gov/gdem.asp⟩; 2012.
[53] DL Elliott, MN Schwartz. Wind energy potential in the United States, PNL-SA-23109, Pacific Northwest Laboratory, Ritchland, WA, USA; September 2013 1993.
[54] EA DeMeo. Renewable energy technology characterizations, EPRI, Palo Alto, CA TR-109496; December 1997.
[55] EEA. Europe's onshore and offshore wind energy potential: an assessment of environmental and economic constraints, European Environment Agency, Copenhagen; September, 2009.